*Laser and Particle Beams* (2015), *33*, 481–487.

doi:10.1017/S026303461500052X

# Amplification of filamentation instability by negative hydrogen ions stream driven by a magnetized counterstreaming $e$–$H^-$ plasmas

MOHAMMAD GHORBANALILU AND BABAK SHOKRI
Physics Department, Shahid Beheshti University, G.C., Tehran, Iran
(Received 10 March 2015; Accepted 20 April 2015)

**Abstract**

The main purpose of this theory is to present a simple picture of magnetic field generation by a relativistic equilibrium counterstreaming electron–negative hydrogen ion ($e$–$H^-$) plasmas propagating parallel to an ambient external magnetic field. The existence of such kind of plasma flows can be imagined during the negative hydrogen ion propagation through neutralizing plasma, in order to generate an energetic neutral hydrogen beam. The produced magnetic field deflects the electron and negative hydrogen ion flows and reduces the efficiency of hydrogen neutral beam generation. We focused our analysis on the influences of the negative hydrogen ion contribution, the particles thermal velocity and the external magnetic field on the growth rate of generated sheared magnetic field. The dispersion relation is obtained using a relativistic two-fluid model and Maxwell equations. The analytical and numerical solutions admit generation of a purely growing transverse electromagnetic field across the ambient external magnetic field. It is shown that $H^-$ current filaments are responsible for deep penetration of the sheared magnetic fields into plasma, however, applying a weak magnetic field $\omega_{ce}^2 \ll \omega_{pe}^2$ suppresses magnetic field generation for a counterstreaming $e$–$H^-$ plasma in the absence of $H^-$ ions dynamics. On the other hand, a magnetic field exists with a small growth rate for strongly magnetized ($\omega_{ce}^2 \gg \omega_{pe}^2$) $e$–$H^-$ plasma when the influence of $H^-$ ions is included. Although the growth rate is small, we expect that magnetic field generation is further amplified and the penetration depth is increased owing to $H^-$ ions stream, on a time scale much longer than the plasma period $t \gg \omega_{pe}^{-1}$.

**Keywords:** Electron beams; Filamentation instability; Magnetized plasma; Two-fluid model

## 1. INTRODUCTION

It is widely believed that the high-energy astrophysical beams, such as gamma ray burst or supernova remnants, emit non-thermal radiations (Kennel & Petschek, 1967; Fonseca *et al.*, 2003; Schlickeiser & Shukla 2003). This fundamental phenomenon was first reported by Erich Weibel, who predicted the generation of strong magnetic fields in plasmas fulled by free energy stored in the temperature anisotropy (Weibel, 1959). He analyzed instability process by a bi-Maxwellian distribution function, with temperature anisotropy ($u_0 \neq u_z$), as

$$f_0(v_0, v_z) = \frac{n}{u_0^2 u_z (2\pi)^{3/2}} \exp\left[-\frac{v_0^2}{2u_0^2} - \frac{v_z^2}{2u_z^2}\right], \quad (1)$$

where $v_0 = (v_x^2 + v_y^2)^{1/2}$ and $v_z$ are velocity components in $x$–$y$ plane and $z$-direction; $u_0^2$ and $u_z^2$ are corresponding temperatures, respectively. He could show that a purely transverse electromagnetic instability was generated when $u_0 \gg u_z$. Later in the same year, a very closely related instability was discovered by Fried that was driven by momentum anisotropy with a distribution function as the form (Fried, 1959)

$$f_0(\mathbf{v}) = \delta(v_y)\delta(v_z^2 - a^2)\delta(v_x). \quad (2)$$

According to the Fried theory, a beam–plasma system turns unstable against electromagnetic modulation normal to the plasma flow ($k \perp v_b$). This instability is often called as the current filamentation (CF) or Weibel-like instability. While in a laser–plasma context, the CF instability is usually identified with the Weibel instability (Califano *et al.*, 2006), it is revealed that the filamentation mode is transverse when both beams are strictly identical (Pegoraro *et al.*, 1996; Tzoufras

Address correspondence and reprint requests to: Mohammad Ghorbanalilu, Physics Department, Shahid Beheshti University, Evin, Tehran, Iran. E mails: mh_alilo@yahoo.com and m_alilu@sbu.ac.ir

*et al.*, 2006; Fiore *et al.*, 2006; Bret *et al.*, 2007; Hao *et al.*, 2008; 2009; Yalinewich & Gedalin, 2010). On the other hand, the Weibel instability develops from a temperature anisotropy and exists in the presence or absence of any beam. Consequently, the CF instability is "beam based", while the Weibel instability is "temperature anisotropy based".

The existence of Weibel and CF instabilities was approved not only in astrophysical but also in laboratory plasmas as well. For instance in streaming and counterstreaming plasma flows (Brian Yang *et al.*, 1993; Califano *et al.*, 2001; Bret *et al.*, 2005; 2006; Shukla & Shukla, 2007; Tautz & Sakai, 2007; Lazar, 2008; Liu *et al.*, 2009; Abraham-Shrauner, 2010; Lazar *et al.*, 2010; Ghorbanalilu *et al.*, 2014) microwave discharge of neutral gases and laser produced plasmas (Bendib *et al.*, 1998; Okada *et al.*, 1999; Ghorbanalilu, 2006; 2011; 2013; Quinn *et al.*, 2012). In addition, on the basis of computer simulation, a strong magnetic field can be generated due to colliding electron clouds in an unmagnetized electron–ion plasma (Sakai *et al.*, 2004). On the other hand, in the recent simulation performed for the interaction between electron–ion plasma flows with a magnetized plasma, the role of heavy ions on the Weibel instability was discussed, in detail (Ardaneh *et al.*, 2014). It was shown that the ions form the current filaments that are the sources of deeply penetrating of the sheared magnetic field into the plasma. Furthermore, the filamentation instability was investigated for counterstreaming electron–proton plasma flows as a main mechanism of collisionless shocks generation (Bret, 2013; 2014). Moreover, in the recent experiment, the CF instability was observed and studied in a laboratory environment (Allen *et al.*, 2012).

It is well known to initiate nuclear fusion, the fusion fuel, must be heated to over 100 million degrees centigrade. This is accomplished, for example, by injecting fast neutralized hydrogen particles into the plasma. The positively charged hydrogen particles have been used exclusively up to now in the heating systems. Therefore, electrons are removed from neutral hydrogen and the positively charged hydrogen ions are then accelerated by electric fields to the required energy. The hydrogen ion beam should be neutralized because charged particles would be deflected by the magnetic field of the plasma cage. To do this purpose the ions have to pass through a cell containing gas or plasma-neutralizer. As a result the ions regain the missing electron from the gas and can be injected as fast neutrals into the plasma. To get a more efficient neutral beam it is necessary to use negative hydrogen ions instead of positive ones, which are easy to be neutralized at high velocities. In this case the dominant role of positive charges is the neutralizing of $H^-$ ions. However, the additional electron, which is responsible for the negative charge of the hydrogen particles, is only loosely bounded and is accordingly readily lost. Therefore, the plasma-neutralizer efficiency is not 100% and a complete neutralization has not been available so far. In this paper the filamentation instability due to the counterstreaming of $e$–$H^-$ plasmas suggested as a mechanism which may play an important role in conversion-efficiency of a neutral hydrogen beam. This means that, if the filamentation of $H^-$ beam occurs before its neutralization, the hydrogen ions are deflected by the self-generated magnetic field and thrown out from the beam line. In the course of this paper, we focus our attention on the instability process and the neutral beam generation does not cover the goal of this investigation.

We use a simple relativistic two-fluid model and Maxwell equations to derive the dispersion equation. The obtained dispersion equation can be easily generalized to other types of plasma systems such as $e$–$e$ and $e$–$i$ plasma flows. We show that ions dynamics plays an important role in the instability process and deep penetration of the generated magnetic field into the plasma. Although the heavy $H^-$ ions have a minor contribution on the instability growth rate, this contribution remains unchanged even in the presence of very strong external magnetic fields. Therefore, it is plausible on a time scale much longer than the plasma period $t \gg \omega_{pe}^{-1}$ that the sheared magnetic field becomes strong enough to deflect the electron filaments and amplifies the CF instability. On the other hand, the numerical analysis shows that the instability growth rate is decreased by increasing the particles thermal velocity. Moreover, the instability happens just in a finite interval of wavenumbers depending on the ratio of the electron thermal velocity to the drift velocity.

The organization of the present paper is as follows. In Section 2, by making use of relativistic two-fluid model and Maxwell equations a general dispersion relation is obtained for counterstreaming $e$–$H^-$ plasma propagating parallel to an ambient external magnetic field. In Section 3, the dispersion relation is solved for two limiting cases: (a) Cold unmagnetized counterstreaming $e$–$H^-$ plasma (b) cold and magnetized counterstreaming $e$–$H^-$ plasma propagating parallel an ambient external magnetic field, when the influence of heavy $H^-$ ions is ignored in the instability process. For both cases the solutions admit generation of a purely growing electromagnetic wave, however, the external magnetic field sufficiently suppresses instability growth. In order to get a complete solution we solved the dispersion relation numerically. The numerical solution allows to consider the influences of the external magnetic field, the contribution of ion filaments, and the particles thermal velocity on the instability process. The results for analytical and numerical solutions are in good agreement. Finally, a summary and conclusions are given in Section 4.

## 2. TWO-FLUID MODEL AND DISPERSION EQUATION

Let us consider a two-component plasma with charge species $\alpha$ ($\alpha = e, H^-$) counterstreaming relativistically with velocity $v_{0z\alpha}$ along an external magnetic field $B_0\hat{e}_z$, where $\hat{e}_z$ is the unit-vector along the $z$-axis in a Cartesian coordinate system and $B_0$ indicates the strength of the external magnetic field. If charge species flow with the same velocity and opposite directions along the external magnetic field, the

https://doi.org/10.1017/S026303461500052X Published online by Cambridge University Press

distribution function for charge species will be given by Eq. (2). We assume that the electromagnetic perturbation is an extraordinary mode in which the magnetic and electric fields perturbations are along the $y$- and $z$-axes, respectively. In this case the extraordinary mode propagates along the $x$-axis ($k \perp B_0$). We expect that a finite density perturbation is excited owing to cross–coupling of the external magnetic field $B_0$ and the sheared magnetic field perturbation. The relativistic momentum equation which is governed on charge particle dynamics is given as

$$\begin{aligned} \frac{d(\gamma_\alpha m_\alpha \vec{v})}{dt} &= \vec{F}_\alpha(t), \\ \frac{d\gamma_\alpha}{dt} &= \frac{\gamma_0^3 \vec{v}}{c^2} \cdot \frac{d\vec{v}}{dt}, \end{aligned} \tag{3}$$

where $\vec{F}_\alpha(t)$ defines all the forces acting on charge particle α and $\gamma_\alpha = (1 - v^2/c^2)^{-1/2}$ is the relativistic gamma factor. Here $v = (v_\alpha^2 + v_{0z\alpha}^2)^{1/2}$, in which $v_\alpha$ is particle fluid velocity and $\gamma_0 = (1 - v_{0z\alpha}^2/c^2)^{-1/2}$ is zero order of relativistic gamma factor. Therefore, to analyse the problem in the linear regime, it is sufficient to describe the charge particles dynamics using the Eq. (3), Maxwell and continuity equations and Faraday's law as below:

$$\frac{\partial n_\alpha}{\partial t} + n_{0\alpha} \frac{\partial v_{x\alpha}}{\partial x} = 0, \tag{4}$$

$$\frac{\partial v_{x\alpha}}{\partial t} = -\frac{e_\alpha B_y}{m_\alpha \gamma_0 c} v_{0z\alpha} + \frac{\omega_{c\alpha}}{\gamma_0} v_{y\alpha} - \frac{1}{m_\alpha \gamma_0 n_{0\alpha}} \frac{\partial p_\alpha}{\partial x}, \tag{5}$$

$$\frac{\partial v_{y\alpha}}{\partial t} = -\frac{\omega_{c\alpha}}{\gamma_0} v_{x\alpha}, \tag{6}$$

$$\frac{\partial v_{z\alpha}}{\partial t} = -\frac{e_\alpha}{m_\alpha \gamma_0^3} E_z, \tag{7}$$

$$\frac{\partial B_y}{\partial x} = \frac{4\pi}{c} \sum_\alpha e_\alpha n_\alpha v_{0z\alpha} + \frac{4\pi}{c} \sum_\alpha e_\alpha n_{0\alpha} v_{z\alpha} + \frac{1}{c} \frac{\partial E_z}{\partial t}, \tag{8}$$

$$\frac{\partial B_y}{\partial t} = c \frac{\partial E_z}{\partial x}, \tag{9}$$

where $n_{0\alpha}$ is the charge density of relativistic particles, $v_{x\alpha}$, $v_{y\alpha}$, and $v_{z\alpha}$ are the components of fluid velocities, and $n_\alpha$ is the small ($n_\alpha \ll n_{0\alpha}$) density perturbation. Furthermore, $E_z$ and $B_y$ are the electric and magnetic fields corresponding to the electromagnetic perturbations, $e_\alpha$, $m_\alpha$, and $c$ are charge density, rest mass, and speed of light, respectively; $\omega_{c\alpha} = e_\alpha B_0/m_\alpha c$ is Larmor frequency. Note that the terms arise from $d\gamma_\alpha/dt$ in Eqs. (5) and (6) are nonlinear and ignored, however, this term come into play just in $z$ component of equation of motion in Eq. (7). Using Eqs. (5) and (6) and the continuity Eq. (4) along with $p_\alpha = k_B n_\alpha T_\alpha$ (where $k_B = 1.38 \times 10^{-23}$ jK$^{-1}$ is Boltzmann constant), we easily get

$$\left( \frac{\partial^2}{\partial t^2} + \frac{\omega_{c\alpha}^2}{\gamma_\alpha^2} - \frac{k_B T_\alpha}{m_\alpha \gamma_\alpha} \frac{\partial^2}{\partial x^2} \right) n_\alpha = \frac{e_\alpha n_{0\alpha} v_{0z\alpha}}{m_\alpha \gamma_\alpha c} \frac{\partial B_y}{\partial x}. \tag{10}$$

It is found from Eq. (10) that the electromagnetic fields $E_z$ and $B_y$ are coupled with density perturbations in the presence of the external magnetic field and the pressure gradient of charged particles. We assume that the perturbations quantities behave sinusoidally and are proportional to $e^{(ikx-\omega t)}$ (where $k$ and ω are the wavenumber and frequency). Consequently, by making use of the linearization procedure for coupled Eqs. (8)–(10), we arrive to the following dispersion relation for small perturbations propagating across the external magnetic field

$$\begin{aligned} 1 - \frac{\omega^2}{c^2 k^2} + \sum_\alpha \frac{\omega_{p\alpha}^2}{c^2 k^2 \gamma_0^3} \\ + \sum_\alpha \frac{\omega_{p\alpha}^2 v_{0z\alpha}^2}{c^2 \gamma_0 [\omega^2 - (\omega_{c\alpha}^2/\gamma_0^2) - (k^2 v_{th\alpha}^2/\gamma_0)]} = 0, \end{aligned} \tag{11}$$

where $v_{th\alpha} = \sqrt{(k_B T_\alpha/m_\alpha)}$ is the thermal velocity of charge particle α. It should be noted that α is running over electron and $H^-$ for $e$–$H^-$ plasma in Eq. (11). In the next section we are going to solve dispersion Eq. (11) and analyze the stability of plasma.

## 3. STABILITY ANALYSIS

We suppose the electron and negative hydrogen ion beams are strictly identical, that is, have the same density and equal drift velocity in opposite directions ($v_{0ze} = -v_{0zi} = v_0$), so the net current is zero. If we expand the dispersion relation (11) over α for electron and $H^-$, we get

$$\begin{aligned} &\left[ z^2 - x^2 + \frac{(1+\eta)}{\gamma_0^3} \right] \left( x^2 - \frac{y^2}{\gamma_0^2} - \frac{z^2 \beta^2 \delta_e^2}{\gamma_0} \right) \\ &\left( x^2 - \frac{y^2 \eta^2}{\gamma_0^2} - \frac{z^2 \beta^2 \delta_e^2 \eta}{\gamma_0} \right) + \frac{z^2 \beta^2}{\gamma_0} \left( x^2 - \frac{y^2 \eta^2}{\gamma_0^2} - \frac{z^2 \beta^2 \delta_e^2 \eta}{\gamma_0} \right) \\ &+ \frac{z^2 \beta^2 \eta}{\gamma_0} \left( x^2 - \frac{y^2}{\gamma_0^2} - \frac{z^2 \beta^2 \delta_e^2}{\gamma_0} \right) = 0, \end{aligned} \tag{12}$$

where $x = \omega/\omega_{pe}$, $z = kc/\omega_{pe}$, $\beta = v_0/c$, $y = \omega_{ce}/\omega_{pe}$, $\delta_e = v_{the}/v_0$, $\eta = m_e/m_i$, are dimensionless parameters, and $\omega_{pe} = (4\pi n_{0e} e^2/m_e)^{1/2}$ is the electron plasma frequency.

### 3.1. Analytical Solution

Equation (12) shows a relation in the sixth order of variable $x$, so it is impossible to find the roots of $x$ analytically. However it is possible to write the Eq. (12) as a third order polynomial in the variable $x^2$, the analytical solution of this equation is

https://doi.org/10.1017/S026303461500052X Published online by Cambridge University Press

very complicate. In spite of all that, for some limiting cases we can find a simple analytical solution.

### 3.1.1. *Cold and Unmagnetized Counterstreaming* e–H$^-$ *Plasmas*

In this case we consider the cold and unmagnetized plasma regime. By substituting $\delta_e = 0$ and $y = 0$ in Eq. (12) we get a fourth order equation for $x$ as below

$$x^4 - \left[z^2 + \frac{(1+\eta)}{\gamma_0^3}\right]x^2 - \frac{\beta^2 z^2}{\gamma_0}(1+\eta) = 0. \tag{13}$$

Solving Eq. (13), we find out a purely growing electromagnetic wave with the growth rate as

$$\Im\omega = \frac{1}{\sqrt{2}}\left\{\left[(z^2 + \frac{(1+\eta)}{\gamma_0^3}\right]\left\{1 - \left[1 + \frac{4\beta^2 z^2 \gamma_0^5 (1+\eta)}{[(1+\eta) + \gamma_0^3 z^2]^2}\right]^{1/2}\right\}\right\}^{1/2}. \tag{14}$$

### 3.1.2. *Cold and Magnetized Counterstreaming* e–H$^-$ *Plasmas*

The second limiting case which allows to find out an analytical solution for Eq. (12) is related to the cold and magnetized counterstreaming $e$–$H^-$ plasma propagating parallel to an ambient external magnetic field, when the influence of heavy $H^-$ ions is ignored in the instability process. Thus by choosing $\delta_e = 0$ and $\eta = 0$ in Eq. (12) we get

$$x^4 - \left(z^2 + \frac{y^2}{\gamma_0^2} + \frac{1}{\gamma_0^3}\right)x^2 + \left[\frac{y^2}{\gamma_0^2}\left(z^2 + \frac{1}{\gamma_0^3}\right) - \frac{z^2\beta^2}{\gamma_0}\right] = 0, \tag{15}$$

whose solution also admit a purely growing electromagnetic wave with the growth rate as

$$\Im\omega = \frac{1}{\sqrt{2}}\left[\left(z^2 + \frac{y^2}{\gamma_0^2} + \frac{1}{\gamma_0^3}\right)\left\{1 - \left[1 - \frac{(4y^2/\gamma_0^2)[z^2 + (1/\gamma_0^3)] - (4z^2\beta^2/\gamma_0)}{[z^2 + (y^2/\gamma_0^2) + (1/\gamma_0^3)]^2}\right]^{1/2}\right\}\right]^{1/2} \tag{16}$$

when the condition of $y^2 < \gamma_0^4 z^2 \beta^2/(\gamma_0^3 z^2 + 1)$ is satisfied. This means that the strength of the magnetic field should be smaller than a critical value for developing the instability.

## 3.2. Numerical Solution

In this subsection we are going to solve Eq. (12), numerically. This solution allows to analyze the dispersion relation without any limitation. Therefore, we are able to include the influences of thermal particles, ion filaments, and the external magnetic field on the instability process.

Figure 1 plots the normalized growth rate $\gamma = \Im\omega/\omega_{pe}$ of the filamentation instability as a function of the normalized wavenumber $kc/\omega_{pe}$ (or the ratio of the penetration depth $c/\omega_{pe}$ to the wavelength $\lambda = 2\pi/k$) computed numerically from Eq. (12), for cold and unmagnetized counterstreaming $e$–$H^-$ plasma. This figure shows that the instability growth rate is increased by increasing the particles drift velocity. Moreover, in the large wavenumbers limit $k^2c^2 \gg \omega_{pe}^2$, and for weakly relativistic case (small $\beta$) the instability growth rate saturates to $\gamma \to \beta$. Note that Figure 1 does not change with or without the ions contribution, significantly. It may be important to note that the analytical results obtained from Eq. (14) are in excellent agreement with the numerical computation of Eq. (12) plotted in Figure 1.

Physically speaking, when the electron current filaments are created, the magnetic fields grow linearly due to mutual attraction of these filaments. When the current filaments sufficiently close to gather, the force of the pressure gradient becomes important in Eq. (5). Since the terms including $\delta_e$ in Eq. (12) are the result of the pressure gradient effect, the influence of the particles thermal velocity on the instability growth rate is depicted in Figure 2 for $\delta_e = 0.2$. It is seen from this figure that not only the maximum growth rate is decreased, but also the instability happens just for a finite interval of wavenumbers. The numerical solution indicates that the cut-off frequency and the maximum growth rate are decreased with increasing $\delta_e$.

Figure 3 demonstrates the influence of the $H^-$ ions current filaments contribution on the instability growth rate for counterstreaming unmagnetized $e$–$H^-$ plasma. As shown in Figure 3 (point line) the cut-off frequency is extended upon to the large values, when the $H^-$ ion contribution is included. This means that the penetration depth of the sheared magnetic field into the plasma is increased, when the heavy $H^-$ ions begin to get involved in the instability process. As a result, the $H^-$ ions form current filaments that are

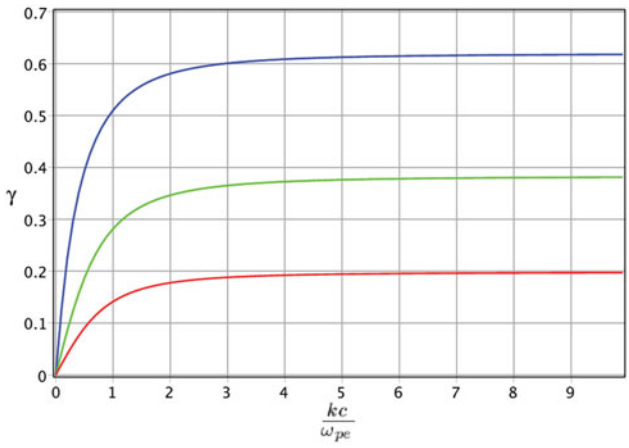


**Fig. 1.** Filamentation instability growth rate as a function of $kc/\omega_{pe}$ for cold and unmagnetized counterstreaming $e$–$H^-$ plasma when the influence of $H^-$ ions is ignored ($\eta = 0$). The red, green, and blue lines are for $\beta = 0.2$, 0.4, and 0.8, respectively.

https://doi.org/10.1017/S026303461500052X Published online by Cambridge University Press

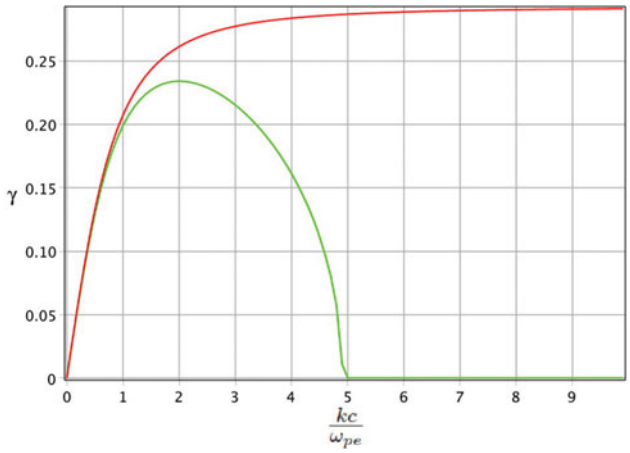


**Fig. 2.** Filamentation instability growth rate as a function of $kc/\omega_{pe}$ for unmagnetized counterstreaming $e$–$H^-$ plasma in the absence of $H^-$ ions contribution for $\beta = 0.3$, computed numerically from Eq. (12). The green and red lines are for $\delta_e = 0.2$ and $\delta_e = 0$, respectively.

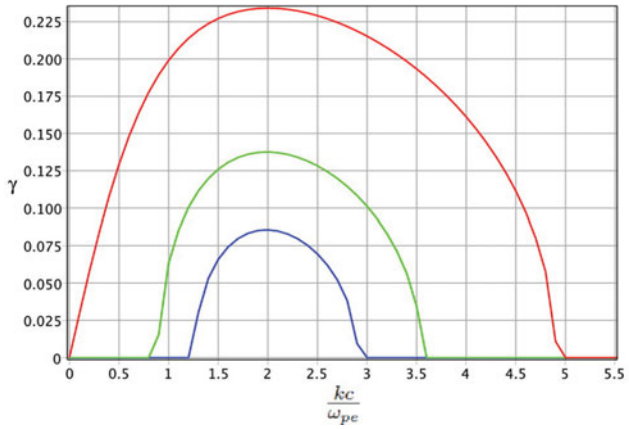


**Fig. 4.** Filamentation instability growth rate as a function of $kc/\omega_{pe}$ for a magnetized counterstreaming $e$–$H^-$ plasma for $\beta = 0.3$, $\delta_e = 0.2$, based on the numerical solution of Eq. (12). The red, green, and blue line are for $\omega_{ce}/\omega_{pe} = 0$, 0.2, and 0.23, respectively.

responsible to the deep penetrating of sheared magnetic into the plasma.

Figure 4 compares the instability growth rate $\gamma = \Im\omega/\omega_{pe}$, for magnetized and unmagnetized counterstreaming $e$–$H^-$ plasma in terms of $kc/\omega_{pe}$. The results show that by applying a magnetic field: (a) The instability growth rate and cut-off frequency are sufficiently decreased, (b) the required threshold wavenumber for the development of the filamentation instability is increased with the increasing magnetic field strength. Hence, the external magnetic field decreases the instability growth rate and constrains further the finite interval of wavenumbers. The results of the analytical and numerical solutions are in good conformity. For example, for parameters $\beta = 0.3$, $\eta = 0$, $\delta_e = 0$, $z = 2$, maximum magnetic field strength for instability development is found around $\omega_{ce} \approx 0.25\omega_{pe}$ from both Eqs. (12) and (16).

In Figure 5 we are going to explain the influence of $H^-$ ions filaments with more detail, in magnetized counterstreaming $e$–$H^-$ plasma. This figure plots the instability growth rate $\gamma = \Im\omega/\omega_{pe}$ as a function of $kc/\omega_{pe}$. The red and green lines are plotted for $\omega_{ce}/\omega_{pe} = 0.23$ in the absence and presence of the $H^-$ ion contribution, respectively. Obviously, the threshold and cut-off frequencies extension are completely perceptible, when the $H^-$ ions filaments come into play. The numerical solution reveals that when the strength of the external magnetic field is increased upon to $\omega_{ce}/\omega_{pe} = 0.3$, the contribution of electrons on the instability development completely lacks. Consequently, the blue line in Figure 5 shows just the $H^-$ ion contribution on the instability process. As shown in Figure 5, although the maximum growth rate is very small, the instability covers a wide range of wavenumbers. Therefore, we expect that the filamentation instability is further amplified and as a result the sheared magnetic field deeply penetrates into the plasma owing to $H^-$ ion streams, on a time scale much longer than the plasma period $t \gg \omega_{pe}^{-1}$.

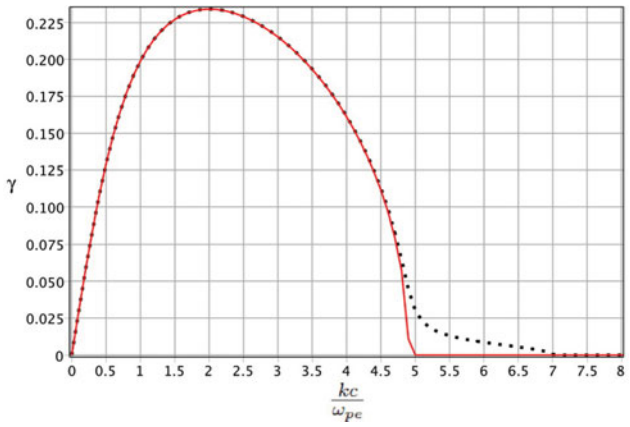


**Fig. 3.** Filamentation instability growth rate as a function of $kc/\omega_{pe}$ for unmagnetized counterstreaming $e$–$H^-$ plasma in the absence [solid line ($\eta = 0$)] and presence of $H^-$ ions contribution [point line ($\eta = 1/1838$)], based on the numerical solution of Eq. (12).

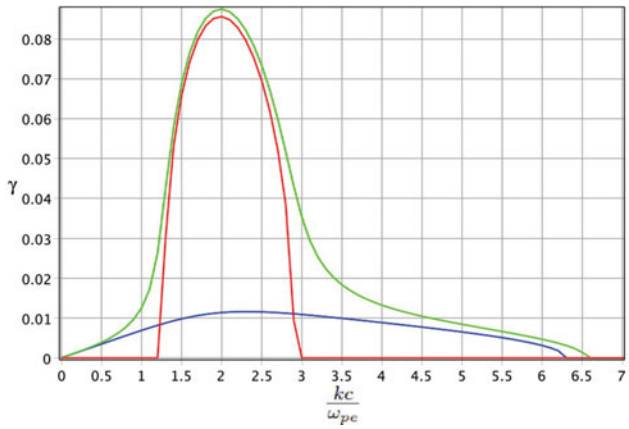


**Fig. 5.** Filamentation instability growth rate for a magnetized counterstreaming $e$–$H^-$ plasma as a function of $kc/\omega_{pe}$ for $\beta = 0.3$, $\delta_e = 0.2$, and $\omega_{ce}/\omega_{pe} = 0.23$. The red and green lines are plotted in the absence ($\eta = 0$) and presence ($\eta = 1/1838$) of $H^-$ ions contribution, respectively. The blue line is for counterstreaming $e$–$H^-$ plasma and $\omega_{ce}/\omega_{pe} = 0.3$.

https://doi.org/10.1017/S026303461500052X Published online by Cambridge University Press

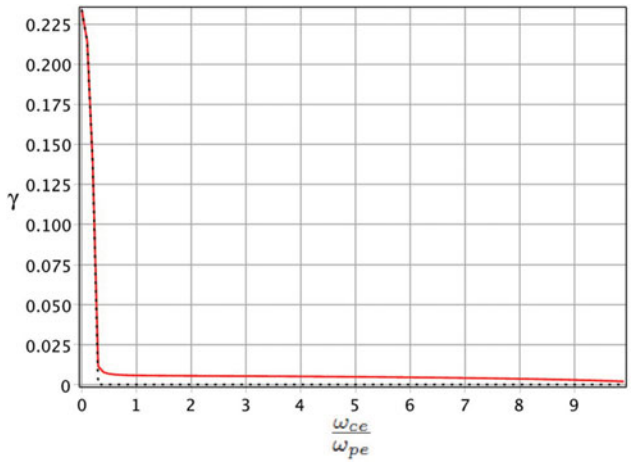


**Fig. 6.** Filamentation instability growth rate for a magnetized counterstreaming $e$–$H^-$ plasma as a function of $\omega_{ce}/\omega_{pe}$ for $\beta = 0.3$, $\delta_e = 0.2$, $kc/\omega_{pe} = 2$. The point and solid lines are plotted in the absence ($\eta = 0$) and presence ($\eta = 1/1838$) of $H^-$ ions contribution, respectively.

The instability growth rate $\gamma = \Im\omega/\omega_{pe}$ in terms of $\omega_{ce}/\omega_{pe}$ is shown in Figure 6, in the presence and absence of the $H^-$ ions contribution. The figure approves our claim that the instability is suppressed by applying a weak magnetic field $\omega_{ce}/\omega_{pe} \approx 0.3$, when the $H^-$ ion contribution is missed. On the other hand, the instability exists with a small growth rate in the presence of a very strong external magnetic field, when the $H^-$ ion filaments get involved. Subsequently, after a long time scale ($t \gg \omega_{pe}^{-1}$) it is possible for the sheared magnetic field to become strong enough to deflect the electrons filaments again and amplifies the instability.

Figure 7 indicates the variation of the instability growth rate $\gamma = \Im\omega/\omega_{pe}$ against $\delta_e = v_{the}/v_0$. Here, we suppose that the temperature of electrons and $H^-$ ions are equal ($v_{thi}/v_{the} = \eta$). As this figure demonstrates for a given external magnetic field, increasing the particles thermal velocity up to the value larger than a critical value can suppress instability generation. We find from this figure that increasing external magnetic field strength reduces this critical value, while it will be increased when the $H^-$ ion contribution gets involved in the instability process (pointed lines).

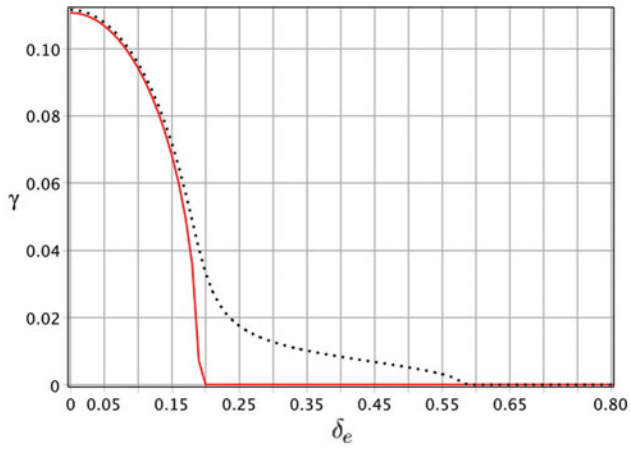


**Fig. 7.** Filamentation instability growth rate for a magnetized counterstreaming $e$–$H^-$ plasma as a function of $\delta_e$ for $\beta = 0.3$, $kc/\omega_{pe} = 2$, $\omega_{ce}/\omega_{pe} = 0.25$. The red and point lines are plotted in the absence ($\eta = 0$) and presence ($\eta = 1/1838$) of $H^-$ ion contribution, respectively.

## 4. SUMMARY AND CONCLUSION

We have discussed the CF instability driven by counterstreaming $e$–$H^-$ plasma propagating parallel to an ambient external magnetic field. We have focused our attention on the influences of the heavy $H^-$ ions contribution, the particles thermal velocity, and the external magnetic field on the instability process. The dispersion relation is derived by using a relativistic two-fluid model and Maxwell equations. We present a analytical solution for two limiting cases (a) cold and unmagnetized counterstreaming $e$–$H^-$ plasma (b) cold and magnetized counterstreaming $e$–$H^-$ plasma propagating parallel to an ambient external magnetic field, when the influence of heavy $H^-$ ions is ignored. In order to obtain a complete solution we solved the dispersion relation numerically. Both numerical and analytical solutions admitted generation of purely growing electromagnetic perturbation across the ambient magnetic field. In addition, both solutions, with same accuracy, approved that for unmagnetized counterstreaming $e$–$H^-$ plasma with non-thermal particles $T_\alpha \to 0$, the instability growth rate saturates to $\gamma \to \beta$ which is in good agreement with previous analytical investigations (Shokri & Ghorbanalilu, 2004*a*; 2004*b*). The stability analysis revealed that when the particles have nonzero thermal velocity $\delta_\alpha \neq 0$ (or $T_\alpha \neq 0$), the maximum growth rate is decreased and an instability develops in a finite interval of wavenumbers. It was shown that when the heavy $H^-$ ions got involved in the instability process, the cut-off frequency was extended. The numerical investigation showed that for a magnetized electron plasma flow: (a) The maximum growth rate and cut-off frequency were decreased, (b) the required threshold wavenumber of filamentation instability development was increased, with increasing magnetic field strength. Consequently, the instability is more constrained by applying an external magnetic field in a finite interval of wavenumbers. The influence of ion filaments was very dominant for magnetized counterstreaming $e$–$H^-$ plasma. It was shown that for a magnetized counterstreaming $e$–$H^-$ plasma, in the absence of role of $H^-$ ion, the CF instability was suppressed by applying a weak external magnetic field ($\omega_{ce}^2 \ll \omega_{pe}^2$). However, the instability occurred with a small growth rate even in the presence of very strong external magnetic fields ($\omega_{ce}^2 \gg \omega_{pe}^2$), when the influence of heavy $H^-$ ions is included. As a result and an important remark, although the growth rate of instability is small for strongly magnetized counterstreaming $e$–$H^-$ plasma, the instability covers a wide range of wavenumbers. This means that the filamentation instability is further amplified and the sheared magnetic field deeply penetrates into the plasma owing to

https://doi.org/10.1017/S026303461500052X Published online by Cambridge University Press

$H^-$ ion streams, on a time scale much longer than the plasma period $t \gg \omega_{pe}^{-1}$ (Ardaneh *et al.*, 2014).

## REFERENCES


Abraham-Shrauner, B. (2010). Weibel instability and quasi-equilibria for collisionless plasmas. *Plasma Phys. Control Fusion* **52**, 025003.

Allen, B., Yakimenko, V., Babzien, M., Fedurin, M., Kusche, K., Muggli, P. (2012). Experimental study of current filamentation instability. *Phys. Rev. Lett.* **109**, 185007.

Ardaneh, K., Cai, D. & Nishikawa, K.H. (2014). Amplification of Weibel instability in the relativistic beam plasma interactions due to ion streaming. *New Astron.* **33**, 1–6.

Bendib, K., Bendib, A., Bendib, K., Bendib, A., Sid, A. & Bendib, K. (1998). Weibel instability analysis in laser-produced plasmas. *Laser Part. Beams* **16**, 473.

Bret, A. (2013). Robustness of the filamentation instability for asymmetric plasma shells collision in arbitrarily oriented magnetic field. *Phys. Plasmas* **20**, 104503.

Bret, A. (2014). Robustness of the filamentation instability in arbitrarily oriented magnetic field: Full three dimensional calculation. *Phys. Plasmas* **21**, 022106.

Bret, A., Christine Firpo, M. & Deutsch, C. (2005). Bridging the gap between two stream and filamentation instabilities. *Laser Part. Beams* **23**, 375.

Bret, A., Christine Firpo, M. & Deutsch, C. (2006). Between two stream and filamentation instabilities: Temperature and collisions effects. *Laser Part. Beams* **24**, 27.

Bret, A., Gremillet, L. & Bellido, J.C. (2007). How really transverse is the filamentation instability? *Phys. Plasmas* **14**, 032103.

Brian Yang, T.-Y., Gallant, Y., Arons, J. & Bruce, A. (1993). Weibel instability in relativistically hot magnetized electron–positron plasmas. *Phys. Fluids B* **5**, 3369.

Califano, F., Attico, N., Pegoraro, F., Bertin, G. & Bulanov, S.V. (2001). Fast formation of magnetic islands in a plasma in the presence of counterstreaming electrons. *Phys. Rev. Lett.* **86**, 5293.

Califano, F., Del Sarto, D. & Pegoraro, F. (2006). Three-dimensional magnetic structures generated by the development of the filamentation (Weibel) instability in the relativistic regime. *Phys. Rev. Lett.* **96**, 105008.

Fiore, M., Silva, L.O., Ren, C., Tzoufras, M.A. & Mori, W.B. (2006). Baryon loading and the Weibel instability in gamma-ray bursts. *Mon. Not. R. Astron. Soc.* **372**, 1851.

Fonseca, R.A., Silva, L.O., Tonge, J.W., Mori, W.B. & Dawson, J.M. (2003). Three-dimensional Weibel instability in astrophysical scenarios. *Phys. Plasmas* **10**, 1979.

Fried, B. (1959). Mechanism for instability of transverse plasma waves. *Phys. Fluids* **2**, 337.

Ghorbanalilu, M. (2006). The Weibel instability on strongly magnetized microwave produced plasma. *Phys. Plasmas* **13**, 102110.

Ghorbanalilu, M. (2011). On the stability analysis of electromagnetic waves along the external magnetic field in a magnetized microwave-produced plasma. *Plasma Phys. Control Fusion* **53**, 035006.

Ghorbanalilu, M. (2013). Resonance and non-resonance Weibel-like modes generation in optical breakdown of a dilute neutral gas by an intense laser field. *Plasma Phys. Control Fusion* **55**, 045002.

Ghorbanalilu, M., Sadegzadeh, S., Ghaderi, Z. & Niknam, A.R. (2014). Weibel instability for a streaming electron, counter-streaming e–e, and e–p plasmas with intrinsic temperature anisotropy. *Phys. Plasmas* **21**, 052102.

Hao, B., Sheng, Z.-M. & Zhang, J. (2008). Kinetic theory on the current-filamentation instability in collisional plasmas. *Phys. Plasmas* **15**, 082112.

Hao, B., Sheng, Z.-M., Ren, C. & Zhang, J. (2009). Relativistic collisional current-filamentation instability and two-stream instability in dense plasma. *Phys. Rev. E* **79**, 046409.

Kennel, C.F. & Petschek, H.E. (1967). Collisionless shock waves in high β plasmas: 1. *J. Geophys. Res.* **72**, 3303.

Lazar, M. (2008). Fast magnetization in counterstreaming plasmas with temperature anisotropies. *Phys. Lett. A* **372**, 2446.

Lazar, M., Dieckmann, M.E. & Poedts, S. (2010). Resonant Weibel instability in counterstreaming plasmas with temperature anisotropies. *J. Plasma Phys.* **76**, 49.

Liu, Y.-H., Swisdak, M. & Drake, J.F. (2009). The Weibel instability inside the electron–positron Harris sheet. *Phys. Plasmas* **16**, 042101.

Okada, T., Sajiki, A. & Satou, K. (1999). Weibel instability by ultraintense laser pulses. *Laser Part. Beams* **17**, 515.

Pegoraro, F., Bulanov, S.V., Califano, F. & Lontano, M. (1996). Nonlinear development of the weibel instability and magnetic field generation in collisionless plasmas. *Phys. Scr. T* **63**, 262.

Quinn, K., Romagnani, L., Ramakrishna, B., Sarri, G., Dieckmann, M.E., Wilson, P.A., Fuchs, J., Lancia, L., Pipahl, A., Toncian, T., Willi, O., Clarke, R.J., Notley, M., Macchi, A. & Borghesi, M. (2012). Weibel-induced filamentation during an ultrafast laser-driven plasma expansion. *Phys. Rev. Lett.* **108**, 135001.

Sakai, J., Schlickeiser, R. & Shukla, P.K. (2004). Simulation studies of the magnetic field generation in cosmological plasmas. *Phys. Lett. A* **330**, 384.

Schlickeiser, R. & Shukla, P.K. (2003). Cosmological magnetic field generation by the Weibel instability. *Astrophys. J.* **599 L57**, 1538.

Shokri, B. & Ghorbanalilu, M. (2004*a*). Relativistic effects on the Weibel instability of circularly polarized microwave produced plasmas. *Phys. Plasmas* **11**, 5398.

Shokri, B. & Ghorbanalilu, M. (2004*b*). Wiebel instability of microwave gas discharge in strong linear and circular pulsed fields. *Phys. Plasmas* **11**, 2989.

Shukla, N. & Shukla, P.K. (2007). Generation of magnetic field fluctuations in relativistic electron–positron magnetoplasmas. *Phys. Lett. A* **362**, 221–224.

Tautz, R.C. & Sakai, J.-I. (2007). Magnetic field amplification in anisotropic counterstreaming pair plasmas. *Phys. Plasmas* **14**, 012104.

Tzoufras, M., Ren, C., Tsung, F.S., Tonge, J.W., Mori, W.B., Fiore, M., Fonseca, R.A. & Silva, L.O. (2006). Space-charge effects in the current-filamentation or Weibel instability. *Phys. Rev. Lett.* **96**, 105002.

Weibel, E.S. (1959). Spontaneously growing transverse waves in a plasma due to an anisotropic velocity distribution. *Phys. Rev. Lett.* **2**, 83.

Yalinewich, A. & Gedalin, M. (2010). Instabilities of relativistic counterstreaming proton beams in the presence of a thermal electron background. *Phys. Plasmas* **17**, 062101.


https://doi.org/10.1017/S026303461500052X Published online by Cambridge University Press